NJC

Accepted Manuscript

This is an *Accepted Manuscript*, which has been through the Royal Society of Chemistry peer review process and has been accepted for publication.

Accepted Manuscripts are published online shortly after acceptance, before technical editing, formatting and proof reading. Using this free service, authors can make their results available to the community, in citable form, before we publish the edited article. We will replace this *Accepted Manuscript* with the edited and formatted *Advance Article* as soon as it is available.

You can find more information about *Accepted Manuscripts* in the **Information for Authors**.

Please note that technical editing may introduce minor changes to the text and/or graphics, which may alter content. The journal's standard **Terms & Conditions** and the **Ethical guidelines** still apply. In no event shall the Royal Society of Chemistry be held responsible for any errors or omissions in this *Accepted Manuscript* or any consequences arising from the use of any information it contains.

Paper

Gold_core - Polyaniline_shell composite nanowires as substrate for surface enhanced Raman scattering and catalyst for dye reduction

Sunil Dutt[1], Prem Felix Siril[1]*, Vipul Sharma[1] and Selvakannan Periasamy[2]

Composite nanowires with gold core (Au_core) and polyaniline shell (PANI_shell) were prepared using swollen liquid crystals (SLCs) as a soft, structure directing template. The composite nanowires were prepared by simply pouring the SLC containing AuCl$_3$ over the SLC containing aniline. SLCs are generally formed by a quaternary mixture containing brine, sodium dodecyl sulphate (SDS) as surfactant, 1-pentanol as co-surfactant and cyclohexane as oil. A portion of cyclohexane was replaced by aniline to make SLCs containing aniline in 10 the oil phase. Similarly, brine was replaced with a solution of gold chloride to make the mesophase containing Au^{3+} ions. Simultaneous chemical oxidation of aniline and reduction of Au^{3+} ions takes place on mixing the above mentioned mesophases, leading to the formation of the nanocomposite. Small spherical nanoparticles or short nanorods that are initially formed get joined together to form nanowires within the PANI shell due to the confinement, typical diffusion path and also due to the strong interaction between Au and PANI. The prepared composite nanowires exhibited good surface enhanced Raman scattering (SERS) for an organic dye. The composite 15 also showed excellent catalytic behavior for the chemical reduction of organic dyes.

1. Introduction

PANI is one of the most common and interesting conducting 20 polymers due to its good environmental stability, ease of synthesis and controllable electrical conductivity through protonation/deprotonation.[1] Polymerization of aniline in general is carried out through oxidative coupling using oxidizing agents such as ammonium persulphate,[2] hydrogen peroxide[3] etc. 25 Research on PANI got renewed vigor recently with the advent of nanotechnology. It has been realized that nanostructuring of PANI can be used as a method to modify and enhance its performance in various applications. Additionally, nanocomposites of PANI with noble metals, carbon 30 nanostructures and metal oxides were found to have superior physical properties that render them potential choices for various applications.[4,5] A number of review articles are available on the preparation of nanocomposites of PANI with metals, metalloids and nonmetals along with exploration of their applications in 35 nanodevices, sensors, catalysis and energy storage.[4] For example, electrocatalytic and sensing properties of PANI/Pt[6,7] and PANI/Pd[8,9] have been studied extensively. Different electrochemical methods were used to synthesize composites of PANI with Pt,[10] Au,[11] Ag[12] and Pd[13]. Some chemical methods 40 were also used to synthesize PANI/metal composites.[4,14] A Major objective of the present work was to develop a novel route for preparing Au-PANI nanocomposite using 'soft' templates.
Synthesis of nanostructured materials often involves the use of structure directing templates.[15] The templates could be 'hard' 45 solids like mesoporous silica, anodized aluminum oxide and polycarbonate membrane. On the other hand 'soft' templates such as micelles that are formed by the self- assembly of surfactants and polymers offer beneficial alternative to the 'hard' templates.

Post-synthesis removal of hard templates needs the use of harsh 50 chemicals.[16,17] Whereas soft templates can be removed by simple washing.[18] SLCs are formed by a quaternary mixture of surfactant, co-surfactant, oil and brine. They can be used as 'soft' templates to prepare noble metal nanostructures.[19,20] Recently, we have used SLCs to prepare 0-D and 1-D nanostructures of 55 PANI.[21,22] Here we report a new synthetic route for the synthesis of Au_core - PANI_shell composite nanowires using SLC templates.

Of late, SERS is increasingly becoming a very useful techniques in different fields such as single molecule detection, biological 60 imaging and to follow catalytic reactions.[23] Different metals can be used as SERS substrates due to their unique ability to interact with light.[24] Tremendous signal amplification in SERS arises due to 'hot spots' in interstitial voids of metal nanoparticles or nanostructures with intersections and high radii of curvature.[25] 65 Au nanostructures with nano-junctions were used in SERS due to their high magnitude of electromagnetic enhancement with good stability and reproducibility.[26,27] Methylene blue (MB) was used as a reporter molecule to test the SERS activity of the Au_core - PANI_shell composite nanowires in the present study.

70 Safe disposal of various harmful and hazardous pollutants is increasingly becoming significant due to stringent regulations.[28] Dyes and other dyestuffs are the major effluents from textile industry that cause significant pollution.[29] Most of these dyes are 75 not biodegradable and persist in the environment.[30] Consumption of hazardous Rhodamine B (Rh B) and harmful MB cause difficult breathing, burning sensation, abdominal and chest pain, severe headache, profuse sweating, mental confusion, painful micturation and methemoglobinemia like syndromes.[31,32] 80 Currently, different methods such as chemical reduction,

photodegradation,[33] reverse osmosis[34] and coagulation[35] are reported in the literature for the safe disposal of these dyes. Chemical reduction using a strong reducing agent is an economical route for the disposal of dyes. Unfortunately, chemical reduction of dyes is a very slow process at ambient conditions. Noble metals such as Au, Pt and Ag are known to catalyse the chemical reduction of dyes. Here we report the very high catalytic activity of the Au_{core}-$PANI_{shell}$ composite nanowires for dye reduction.

2. Experimental section
2.1 Materials
All chemicals for the synthesis were used in the as received condition except aniline from Merck that was vacuum double distilled before use. All other chemicals such as SDS, cyclohexane, MB from Merck, sodium chloride from SD Fine chemicals, 1-pentanol from Loba chemie, gold (III) chloride, rhodamine B (Rh B), sodium borohydride ($NaBH_4$) from Sigma Aldrich were used as received. Ultrapure water from ELGA Pure lab classic (Resistivity 18.2 MΩ-cm) was used to prepare solutions.

2.2 Preparation of the mesophases and Au_{core} - $PANI_{shell}$ nanocomposite
SLCs containing aniline was prepared by following the reported procedure.[22] Typically, SDS (0.4 gm) was first dissolved in the aqueous salted medium (1 ml, 0.1 M NaCl). Further addition of 1.5 ml of a mixture of aniline and cyclohexane (10 % v/v) as swelling oil phase followed by vortex mixing yielded an opaque gel. The co-surfactant (1-pentanol) was then added to the mixture with intermittent vortex mixing to produce the mesophase. The SLC containing gold chloride was also prepared similarly. Note that only the aqueous salted medium (1 ml 0.1 M NaCl) in aniline mesophase was replaced with aqueous gold chloride (1 ml 0.01 M $AuCl_3$) and the oil phase was replaced with pure cyclohexane (1 ml). The prepared mesophases were kept sealed and allowed to equilibrate for few days before further experiments.

Au_{core} - $PANI_{shell}$ nanocomposite was prepared by pouring the gold chloride containing mesophase above the aniline containing mesophase. The mixture was left as such for next 72 h at room temperature for the completion of polymerization. The nanocomposite was easily extracted from the mesophase by the addition of isopropyl alcohol followed by centrifugation. Samples were then washed thoroughly with a mixture of isopropanol and water and dried in a hot air oven at 50 °C for 12 h. A PANI sample was also prepared by following standard procedures without the presence of any template.[36] This sample will be called bulk-PANI hereafter. The properties of the Au_{core} - $PANI_{shell}$ nanocomposite were compared with the properties of this bulk-PANI.

2.3 Characterization of the Au_{core} - $PANI_{shell}$ nanocomposite
UV-Visible absorption spectra of the samples dispersed in water was recorded using Perkin Elmer Lambda-750 Spectrophotometer. Fourier transform Infra-red (FTIR) spectra of the samples were recorded using Perkin Elmer FT-IR spectrometer with a scan rate of 8 in the range of 4000-600 cm^{-1}

and with a resolution of 4 cm^{-1}. Transmission electron microscopy (TEM), scanning TEM (STEM) and energy dispersive X-ray (EDX) analysis of the sample was done using FEI Tecnai G^2 20 S-Twin microscope operating at 200 kV. X-ray photoemission spectroscopy (XPS) was carried out using Thermo K-alpha instrument. Progress of dye reduction was followed by using Shimadzu UV-4250 UV-visible absorption spectroscope.

2.4 SERS experiments
The substrates (1 mg/ml, Au_{core} - $PANI_{shell}$ nanocomposite and bulk-PANI) were dispersed in the aqueous solution of MB (1×10^{-5}M) for 12 h and were drop casted on clean glass slides. MB solution (1×10^{-2} M) without any substrate was also drop casted on clean glass slide. The Raman spectra were recorded using Renishaw inVia micro-Raman using λ=785 nm laser.

2.5 Dye reduction studies
Chemical reduction of MB and RhB dyes using $NaBH_4$ was tested in presence of the nanocomposite as catalysts. The procedure as reported in the literature was followed.[37] In a typical procedure, 0.1 ml (0.5 M) $NaBH_4$ was added to 1 ml (5×10^{-5} M) of Rh B or MB and then progress of the reaction was studied by recording the UV-visible absorption spectra at different time intervals. For dye reduction using the Au_{core} - $PANI_{shell}$ nanocomposite as catalysts, 0.05 ml of the catalyst suspension in water (1 mg/ml) was added into 1 ml (5×10^{-5}M) of Rh B or MB and sonicated it for 5 minutes, then 0.1 ml (0.5 M) $NaBH_4$ was added and progress of the reaction was monitored. Catalytic activity of the nanocomposite was compared with the activity of 1 mg of bulk-PANI.

3. Results and discussion
A mesophase containing aniline and another one containing $AuCl_3$ was prepared and the latter was poured over the former to prepare the Au_{core} - $PANI_{shell}$ nanocomposite. The mesophase containing aniline was transparent, gelatinous, and colorless (Fig. 1a). The mesophase containing gold was also transparent and gelatinous, but was yellow in colour (Fig. 1b). The interface between the two mesophases was distinct on pouring one over the other due to the difference in colour (Fig 1c). A slow, but continuous change in color of the interface between the two occurred with time (Fig. 1d). The interface became greenish-black in color and the thickness of this greenish-black colored band increased progressively to both sides. The entire mesophase became completely greenish-black after nearly 72 hours (Fig. 1e).

Simple mixing of aniline and $AuCl_3$ is reported to yield Au-PANI nanocomposites as a result of the redox reactions.[14] Thus, it appears that simultaneous oxidation of aniline and reduction of Au^{3+} ions led to the formation of the nanocomposite. Such an oxidation-reduction reaction between aniline and Au^{3+} ions is expected to proceed quite quickly. The redox reaction did take place quickly at the interface as we observed the appearance of greenish-black color within few minutes after the addition of gold containing mesophase over the aniline containing mesophase. However, further progress of the reaction was slow as the progress was limited by mass transport of the reactants across the interface. The presence of the Au-PANI nanocomposite at the

interface may be causing the diffusion to slow down
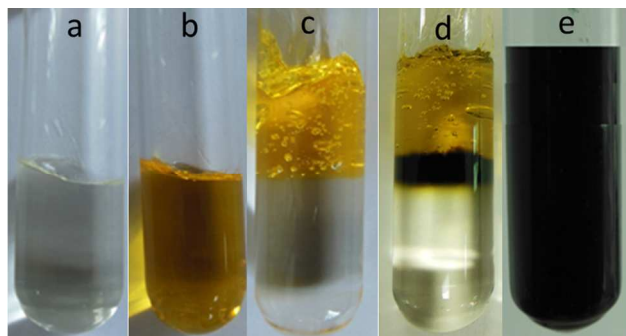
Fig. 1. Photographs of: (a) mesophase containing aniline, (b) mesophase
5   containing gold chloride, (c) mesophases at the time of mixing, (d)
mesophases after 1 h reaction and (e) mesophases after 72 h showing the
completion of reaction.

3.1 Characterisation of the nanocomposite
3.1.1 UV-Visible absorption spectroscopy

10 UV-visible absorption spectra of the nanocomposite and bulk-
PANI dispersed in water are shown in Fig. 2. The spectrum of
Au_{core} - $PANI_{shell}$ composite nanowire exhibited three absorption
peaks at 350 nm, 422 nm and 842 nm. The absorption spectrum
of bulk-PANI was also similar to the composite. These three
15 absorption peaks are characteristic absorption peaks of the
emeraldine oxidation state of PANI.[38, 39] The absorption peaks in
the range of 300-350 nm and at around 422 nm are usually
attributed to π-π* transition of benzenoid rings and localized
polaron transition respectively.[38,39] The peak at 842 nm is due to
20 the π-polaron transition. Presence of this peak indicates that
PANI in the nanocomposite is in the conductive state.[40, 41] No
distinct absorption peak was observed for the surface plasmon
resonance of Au nanostructures. This may be either due to the
overlapping of the absorption band of PANI and SPR of Au or
25 due to the masking of the absorption band of Au by PANI.[42] It is
also to be noted that SPR of metal nanoparticles in general is
highly sensitive to their immediate environment.[41] Masking of
SPR of Au may be happening also due to the complete
encapsulation of Au nanostructures within a shell of PANI.

30
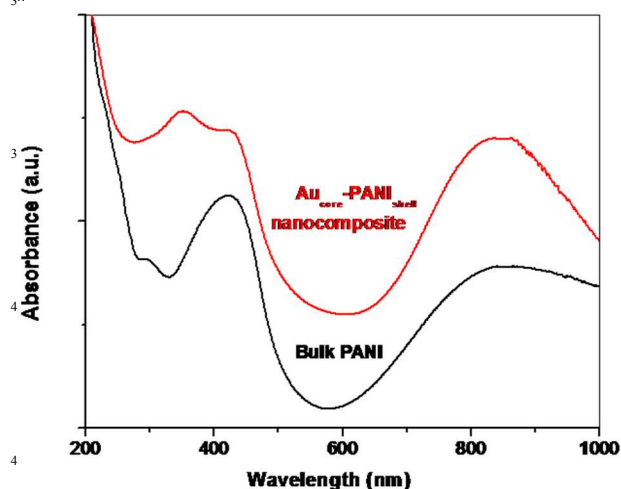
Fig. 2. UV-visible absorption spectra of bulk-PANI and Au_{core} - $PANI_{shell}$
nanocomposites dispersed in water.

3.1.2 FTIR spectroscopy

50 FTIR spectra of bulk-PANI and Au_{core} - $PANI_{shell}$ nanocomposite
prepared in this study are shown in Fig. S1, ESI†. Bulk-PANI
showed main characteristic absorption bands at 3454 cm^{-1} (N-H
stretching band), 1571 cm^{-1} (quinoid ring stretching band), 1485
cm^{-1} (benzenoid ring stretching band), 1299 cm^{-1} (secondary C-
55 N stretching band), 1120 cm^{-1} (vibration band of dopant anion)
and 800 cm^{-1} (para disubstituted benzene rings). The data
matched well with the reported characteristic FTIR data for
doped PANI.[42] Au_{core} - $PANI_{shell}$ nanocomposite showed main
characteristic absorption bands at 3339 cm^{-1}, 1465 cm^{-1}, 1373
60 cm^{-1}, 1305 cm^{-1}, 1128 cm^{-1} and 811 cm^{-1}. Comparison of the
FTIR bands of PANI and the nanocomposite showed that there is
significant shift of bands corresponding to PANI for the
nanocomposite. Such shift of the bands is due to the interaction of
Au and PANI.[5]

65

3.1.3 TEM imaging and EDS analysis
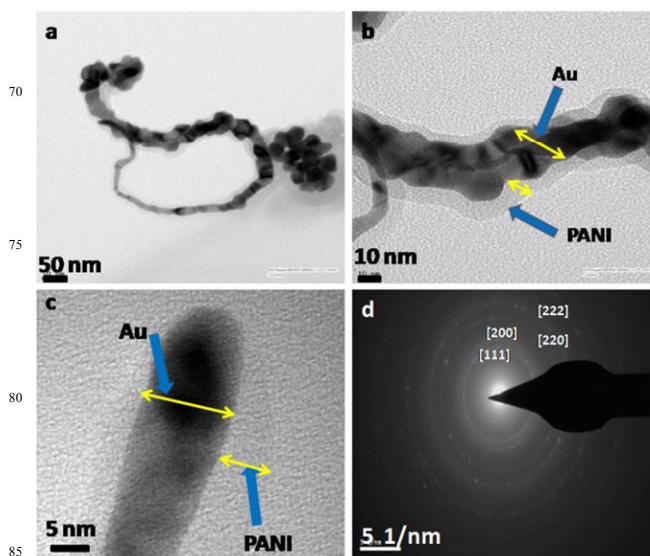
Fig. 3. TEM images Au_{core} - $PANI_{shell}$ nanocomposite prepared using
SLCs. **(a)** long nanowire and some nanoparticles, **(b)** high resolution
image of portion of (a) where the PANI shell is clearly visible, **(c)** end of
90 a nanowire and **(d)** the selected area electron diffraction (SAED) pattern.

TEM imaging showed that the prepared nanocomposite has wire
like morphology as shown in Figures 2 and in S2, ESI†. Some
spherical particles were also observed. The diameter of the wires
95 was typically 5-20 nm and length was in micrometers. The
spherical particles also have diameter in the range of 5-20 nm.
The thin layer of PANI covering the wires and particles was
observed as a halo around them and had thickness in the range of
1-5 nm. The diameter of the wires was non-uniform and the wires
100 appeared to be formed by the joining of spherical particles or
nanorods. Overgrowth of some spherical gold nanoparticles
encapsulated in PANI matrix, on the wires was also seen in some
images (For eg. Fig. 3a). It can be observed from Fig. 2c that the
ends of the nanowires are not capped by PANI. The selected area
105 electron diffraction (SAED) pattern is shown in Fig. 2(d). The
ordered bright diffraction spots in SAED pattern corresponds to

[111] d=0.232 nm, [200] d=0.198 nm, [220] d= 0.136 nm, and [222] d=0.117 nm (CPDS card no. 1780) of Au(0). Energy dispersive X-ray (EDX) analysis of the nanocomposite deposited on TEM grid was also done and data is shown in Fig. S3, ESI†. Three characteristic peaks corresponding to Au element were observed in the EDX spectrum at 0.25 keV, 2.2 keV and 9.7 keV. These correspond to L-series of Au. Peak at 8.9 keV is due to copper grid. Characteristic peak corresponding to nitrogen was also observed confirming the presence of aniline in the nanocomposite. EDS line scan spectra were also recorded across the composite nanowire and is shown in Fig. S4, ESI†. Intensity of the Au-L line is low at the edges of the composite nanowire and the intensity increases towards the core. The intensity of the N-K line remained constant along the line. This also confirmed that the composite indeed has a core-shell structure. EDS elemental mapping of the nanocomposite was also done and the images are shown in Fig. 4. The core-shell nanostructure of the nanocomposite with Au-core and PANI-shell was further confirmed by the elemental mapping.
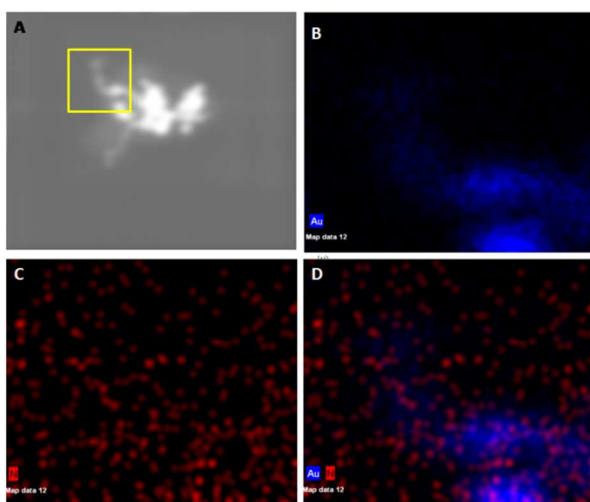
Fig.4. (A) STEM image of Au_{core} - $PANI_{shell}$ nanocomposite. EDS elemental map of: **(B)** Au(LA), **(C)** N(K) **(D)** Au(LA) and N(K) together.

3.1.4 XPS spectroscopy

Au_{core} - $PANI_{shell}$ nanocomposite was further characterized by XPS. XPS spectra of Au_{core} - $PANI_{shell}$ nanocomposite is shown Fig. S5 in the ESI†. A high resolution data in the energy range of 80 eV to 92 eV is shown in in Fig. 5(A). The peaks in XPS spectrum shown in Fig. 5(A) at 83.7 eV ($^4f_{7/2}$) and 87.6 eV ($^4f_{5/2}$) correspond to Au(0) state of gold. The binding energy values matched well with the reported data for PANI-Au composites and confirmed the Au(0) state of elemental gold.[43] The binding energy of 4f electrons of Au was slightly lower in the composite. This is usually attributed to the charge-transfer interactions between Au and PANI in the composite.[43] Absence of peak at 92 eV confirmed that there is no unreacted Au^{3+} ions present in the Au_{core} - $PANI_{shell}$ composite.[5] The N1s core level XPS spectrum (Fig. S5 (b), ESI†)) showed three peaks with binding energies of 399.6 eV (benzenoid amines, -NH-), 401.7 eV (doped imines, N^{+}), 398.1 eV (quinoid amines, =N-).[44] The core level C1s spectrum (Fig. S5 (c), ESI†) matched with the reported data for

conjugated polymers.[44] Also binding energies at 164.5 eV (S^2p) and 230.7 eV (S^2s) confirmed the presence of sulphur.[5] Presence of sulphur is due to the doping of PANI by the surfactant, i.e. $SDS^{21, 22}$.

3.2 Mechanism of formation of the nanocomposite

One-dimensional morphology of Au_{core}-$PANI_{shell}$ nanocomposites is due to the effect of confinement, typical diffusion path of the reactants and the strong interaction between PANI and Au. Au^{3+} ions are located in the aqueous phase and the aniline molecules are mainly located at the oil-water interface.[21,22] Au^{3+} ions diffuse through the aqueous phase towards the aniline containing mesophase, when the two mesophases come in contact with each other. Diffusion of the Au^{3+} ions towards the aniline containing mesophase is clearly evident in the Fig 1c, as we can see the yellow streaks in the aniline containing mesophase. Simultaneously, aniline molecules diffuse through the oil phase towards the gold containing mesophase. Au^{3+} ions and aniline molecules encounter each other and the polymerization takes place in a zipping fashion at the oil-water interface. Simultaneous reduction of Au^{3+} ions lead to the formation of gold seeds. It appears that the polyaniline nanofibrils that are formed initially binds firmly on the surface of gold seeds. The strong interaction between Au and PANI was evident from the FTIR spectra and from the XPS results. This strong interaction may also be responsible for the one dimensional growth of the nanocomposite along with the confinement provided by the template. Further growth of the nanoparticles takes place as more Au^{3+} ions diffuse towards the initially formed nanocomposites.
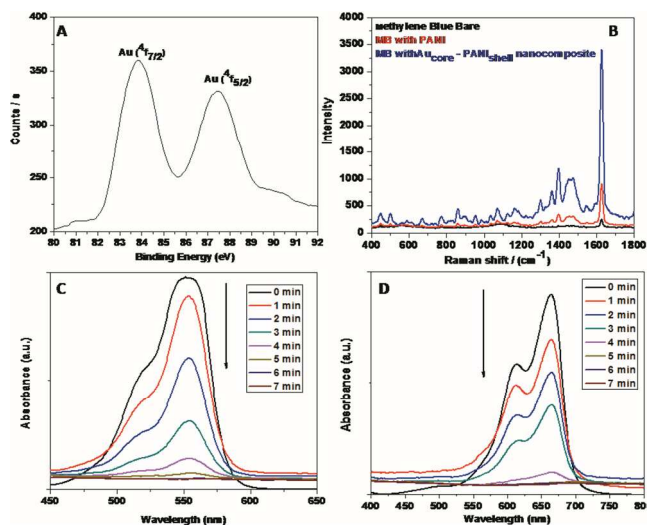
Fig. 5. (A) Au 4f XPS spectrum. **(B)** Raman spectra of MB (10^{-2} M), MB on bulk-PANI substrate and MB on Au_{core}-$PANI_{shell}$ nanocomposite substrate. **(C and D)** Time dependent UV-visible spectra of Rh B and MB showing the progress of dye reduction by $NaBH_4$ in presence of Au_{core} - $PANI_{shell}$ nanocomposite recorded at 1 min intervals.

3.3 SERS studies

MB was used as a reporter molecule to study the SERS activity of the Au_{core} - $PANI_{shell}$ nanocomposite. Raman spectra of MB on Au_{core} - $PANI_{shell}$ nanocomposite is shown in Figure 5(B). Raman spectra of MB alone on glass slide and MB adsorbed on bulk-

PANI is also shown in Figure 5(B). High SERS activity of the nanocomposite is clearly evident from a comparison of the three Raman spectra shown in Figure 5(B). Main Raman peak for MB was observed at 1620 cm^{-1} corresponding to ring stretch (ν CC). The peak at 1396 cm^{-1} signify the symmetric CN stretching (ν-sym CN).[45,46] Peaks at 1164 cm^{-1}, 1037 cm^{-1} (β CH), 861, 668 (γ CH), 449 (δ CNC) of MB were also observed to be enhanced.[45,46] Apart from the Raman peaks corresponding to MB, peaks corresponding PANI were also observed. The small peaks at 1128 cm^{-1} (quinoid rings), 1470 cm[-1](C=N stretching mode of quinoid rings), 1224 cm^{-1} (C-N stretching mode of single bond), 1360 cm^{-1} (C-N[.+] stretching modes of the delocalized polaronic charge carrier) and 1542 cm^{-1} (N–H bending deformation band of protonated amine) also confirmed that Au nanowires are covered with PANI and form Au_{core} - $PANI_{shell}$ type of structure.[47] The enhancement factor (EF) for the main SERS peaks for MB was calculated by using the following equation:[48]

$$EF = \frac{I_{SERS}/C_{SERS}}{I_{RS}/C_{RS}}$$

I_{SERS} = intensity of enhanced spectrum, C_{SERS} = concentration of the dye adsorbed on the substrate, I_{RS}= intensity of the normal Raman spectra and C_{RS} = concentration of normal Raman spectrum. We have quantified the amount of dye adsorbed on the substrates (C_{SERS}) by using UV-visible absorption spectroscopy. UV-visible absorption spectrum of the dye solution was recorded along with the spectra for the supernatant dye solution after mixing with the substrates for 12 hours. The UV-visible spectra are shown in Figure S6, ESI†. The amount of the residual dye present in the supernatant was obtained from a calibration curve generated from the UV spectra of a series of dye solutions with varying concentrations. Thus, the amount of dye adsorbed on bulk-PANI and Au_{core} - $PANI_{shell}$ nanocomposite was estimated to be 1.5x10^{-6} M/mg and 5.8x10^{-7} M/mg respectively. The adsorption experiments were performed under dark conditions to ensure that there is no photoreduction of the dye. Complete decoloration of the dye solution was observed in 12 hours when MB dye was mixed with bulk-PANI for the SERS experiments (Figure S6, ESI†). On the contrary the dye solution was still colored even after mixing the Au_{core} - $PANI_{shell}$ nanocomposite with it for 12 hours. The photographs of the dye solutions before and after the adsorption are also shown in Figure S6, ESI†. PANI and its nanocomposites are reported in the literature as efficient adsorbents for dyes including MB.[49, 50] While bulk-PANI adsorbed almost the entire dye molecules present in the dye solution, the Au_{core} - $PANI_{shell}$ nanocomposite was much less efficient in adsorbing the dyes. The calculated EF for some representative Raman peaks of MB are presented in Table 1.

Table 1. The EF of the major SERS peaks for MB.

	Raman Peak / cm[-1]				
	1620	**1396**	**1164**	**861**	**449**
Bulk-PANI	2.4 x10^{4}	1.7x10^{4}	9.7 x10^{3}	1.1 x10^{4}	9.2x10^{3}
Au_{core}-$PANI_{shell}$	2.4 x10^{5}	1.5 x 10^{5}	6 x10^{4}	7.7 x10^{4}	6.4x10^{4}

Interestingly, it was observed that Raman signals of the reporter molecule were enhanced on the bulk-PANI substrate also. EF of the Au_{core} - $PANI_{shell}$ was however much higher than the EF for bulk-PANI. Bulk-PANI is not known to be a SERS substrate. The Raman enhancement on bulk-PANI must be due to the chemical enhancement arising from the charge transfer between PANI and the dye molecules. The SERS for MB on the Au_{core} - $PANI_{shell}$ nanocomposite was comparable to the typical enhancement on Au nanoparticle surfaces.[46] High EF obtained for the nanocomposite substrate shows that the reporter molecules are able to diffuse through PANI shell to reach closer to the surface of Au nanowires. Because the Raman enhancement decreases exponentially with the distance between the substrate and reporter molecules.[51] The increase in SERS signal for the nanocomposite substrate may be due to the presence of hot spots as well as due to chemical enhancement by the PANI shell. Additionally the Au_{core} - $PANI_{shell}$ nanocomposite offers the possibility to enrich the presence of reporter molecules in the vicinity of the underlying gold nanowire substrate due to the unique morphology of the nanocomposite.

3.4 Catalytic activity for dye reduction

Catalytic activity of the prepared Au_{core}- $PANI_{shell}$ nanocomposite for the reduction of organic dyes was studied with the help of UV-visible absorption spectra. The catalytic reduction of MB and Rh B was tested following the procedure reported earlier.[52] Time-resolved UV-visible absorption spectra of Rh B and MB in presence of the catalysts and the reducing agent is shown in Fig. 5(C) and 5(D) respectively. Progress of the reduction of Rh B and MB is evident in Fig. 5(C) and 5(D) in the form of decrease in the intensity of absorbance maximum at λ_{max} - 554 nm (characteristic absorption band of Rh B) and at λ_{max} - 665 nm (characteristic absorption band of MB) with time. The characteristic peaks for the dyes disappeared completely after 5 min, indicating the completion of the reaction. The bright coloured dye solution became almost colourless in 5 min as shown in Figure S7, ESI†. The reduction of dyes was negligible in absence of the catalysts in 7 min. The dye reduction data fitted well in a linear plot of -ln (C_t/C_o) versus reduction time. C_t and C_o are concentrations of the dye at time t and t_0 respectively. The reaction thus follows the first order kinetics as reported earlier.[53] The kinetic curves for the reductive degradation of RhB and MB in presence and absence of the catalyst and comparison of first-order rates are shown in Figure S8 (a and b), ESI†. The rate constant (k, min[-1]) was obtained from the linear plot and found to be, k (Rh B) = 0.378 s^{-1}, k (MB) = 0.42 s^{-1} which is higher than reported values with gold nanoparticles.[52] A comparison of the catalytic activities of various catalysts for the chemical reduction of Rh B and MB is given in Table 2. It is clearly evident from the Table 2 that the Au_{core} - $PANI_{shell}$ nanocomposite outperformed other catalysts that are reported in the literature.

It is reported in the literature that the reduction of dye will not proceed even in excess of $NaBH_4$ without any catalyst.[37] Since, the nanocomposite contains PANI and Au, we have also checked the catalytic activity of bulk-PANI. The data reported in Figure S8, ESI† clearly revealed that bulk-PANI did not catalyze the dye reduction reaction. Thus, it is clear that the catalytic activity of the nanocomposite is only due to the presence of gold. Noble

metal nanostructures can act as an electron relay in redox reactions.[37] The electrons are donated by $NaBH_4$ to Au and the dye molecules capture the electrons from Au.[37] The adsorption of the reactant molecules on the catalyst surface is required for the promotion of the electron relay. It is already established that the PANI shell helps to enrich the dye concentration around the Au nanowire in the composite. This may be the reason for enhanced catalytic activity of the nanocomposite over Au nanoparticles.

Table 2. A comparison of catalytic activities of different catalysts that are reported in the literature with the Au_{core} - $PANI_{shell}$ composite nanowires for the chemical reduction of MB and Rh B.

Sr. No.	Catalyst	$T_{completion}$ Rh B / min	$T_{completion}$ MB / min	Ref.
1	Au-loaded Fe_3O_4@C composite microspheres		10	53
2.	Ag nanoparticles on Silica spheres		7.5	54
3.	Fe_3O_4@PANI@Au Nanocomposites	18		37
4.	Au-PANI nanocomposite	15		52
5.	Au_{core} - $PANI_{shell}$	6	5	This work

4. Conclusions

Novel nanocomposite having Gold-core and polyaniline-shell with nanowires morphology can be effectively prepared by using swollen liquid crystals as 'soft' templates. The formation of such a nanocomposite is due to the tight confinement and typical diffusion path offered by the mesophases and the strong chemical interaction between polyaniline and the surface of Gold nanoparticles. The unique morphology of the nanocomposite enables it to have very good surface enhanced Raman scattering (SERS) activity due to the presence of nanojunctions and due to the ability of the polyaniline shell to adsorb small molecules. Infact, SERS on the nanocomposite was not expected to be similar to typical Gold surfaces as the Gold nanoparticles are encapsulated in a thin polyaniline shell. Interestingly, it was discovered serendipitously that polyaniline can act as a good SERS substrate for reporter molecules such as methylene blue. SERS enhancement by polyaniline is due to its ability to adsorb molecules such as methylene blue leading to chemical enhancement of Raman spectrum. The prepared nanocomposite can also be used as an efficient catalyst for the reduction of organic dyes. The nanocomposite can have practical applications in effluent treatment due to its high catalytic activity. The facile synthesis approach reported in this paper opens up a new window for the preparation of such unique nanocomposites with other metals and conducting polymers.

Notes and references

1School of Basic Sciences, Indian Institute of Technology Mandi -175005, Himachal Pradesh, India.

2Center for Advanced Materials and Industrial Chemistry, School of Applied Sciences, RMIT University, Australia.

*Email: prem@iitmandi.ac.in, Tel. no: +91-1905300040 Fax: +91-1905237942

†Electronic Supplementary Information (ESI) available: See DOI: 10.1039/b000000x/
FTIR spectra, HR-TEM images, EDX spectrum, XPS overall spectrum and N1s, C1s core level spectra, Dye adsorption data and photograps of dye solution before and after adsorption, images of UV cuvettes before and after dye reduction, kinetic curve and comparison of first-order rates of reductive degradation of MB and Rh B dyes are shown in supplementary information.

1. W. Jia, L. Su and Y. Lei, *Biosensors and Bioelectronics,* 2011, **30**, 158.
2. J. M. Yeh, S. J. Liou, C. Y. Lai and P. C. Wu, *Chem. Mater.,* 2001, **13**, 1131.
3. Z. Chen, C. D. Pina, E. Falletta, M. L. Faro, M. Pasta, M. Rossi and N. Santo, *Journal of Catalysis,* 2008, **259**, 1.
4. G. C. Marjanovic, *Synth. Met.*, 2013, **170**, 31.
5. J. M. Kinyanjui, D. W. Hatchett, J. A. Smith and M. Josowicz, *Chem. Mater.,* 2004, **16**, 3390.
6. A. Kitani, T. Akashi, K. Sugimoto and S. Ito, *Synth. Met.,* 2001, **121**, 1301.
7. Z. R. Zhang, W. F. Bao and C. C. Liu, *Talanta,* 1994, **41**, 875.
8. M. Hasik, A. Drelinkiewicz, M. Choczynski, S, Quillard and A. Pron, *Synth. Met.*, 1997, **84**, 93.
9. E. T. Kang, Y. P. Ting, K. G. Neoh and K. L. Tan, *Synth. Met.*, 1995, **69**, 477.
10. K. M. Kost, D. E. Bartak, B. Kazee and T. Kuwana, *Anal. Chem.*, 1988, **60**, 2379.
11. D. W. Hatchett, M. Josowicz, J. Janata and D. R. Baer, *Chem. Mater.,* 1999, **11**, 2989.
12. Y. Gao, D. Shan, F. Cao, J. Gong, X. Li, H. Ma, Z. Su, and L. Qu, *J. Phys. Chem. C,* 2009, **113**, 15175.
13. K. Mallick, M. Witcomb and M. Scurrell, *Platinum Metals Rev.*, 2007, **51(1)**, 3.
14. Y. F. Huang, Y. I. Park, C. Y. Kuo, P. Xu, D. J. Williams, J. Wang, C. W. Lin and H. L. Wang, *J. Phys. Chem. C* , 2012, **116**, 11272.
15. T. L. Wade and J. E. Wegrowe, *Eur. Phys. J. Appl. Phys.*, 2005, **29**, 3.
16. C. R. Martin, L. S. V. Dyke, Z. Cai and W. Liang, *J. Am. Chem. Soc.*, 1990, **112**, 8976.
17. H. D. Tran, D. Li and R. B. Kaner, *Adv. Mater.,* 2009, **21**, 1487.
18. L. Ramos and P. Fabre, *Langmuir,* 1997,**13**, 682.
19. P. F. Siril, A. Lehoux, L. Ramos, P. Beaunier and H. Remita, *New J. Chem.* 2012, **36**, 2135.
20. P. F. Siril, L. Ramos, P. Beunier, P. Archirel, A. Etcheberry and H. Remita, *Chem. Mater.*, 2009, **21**, 5170.
21. S. Dutt and P. F. Siril, *Mater. Lett.*, 2014, **124**, 50.
22. S. Dutt and P. F. Siril, *J. Appl. Polym. Sci.,* 2014,**131**, 40800.
23. W. Xie and S. Schlucker, *Phys. Chem. Chem. Phys.*, 2013, **15**, 5329.
24. X. Wang, W. Shi, G. She and L. Mu, *Phys. Chem. Chem. Phys.*, 2012, **14**, 5891.
25. H. Zhu, M. L. Du, M. L. Zou, C. S. Xu and Y. Q. Fu, *Dalton Trans.*, 2012, **41**, 10465.
26. Y. Zhang, S. Sun, D. Deng, X. Song, B. Ding and Z. Yang, *Cryst. Eng. Comm.*, 2012, **14**, 656.

New Journal of Chemistry Accepted Manuscript

27. J. Xie, Q. Zhang, J. Y. Lee and D. I. C. Wang, *ACS Nano*, 2008, **2(12)**, 2473.

28. J. Zhao, T. Wu, K. Wu, K. Oikawa, H. Hidaka and N. Serpone, *Environ. Sci. Technol.*, 1998, **32**, 2394.

29. I. K. Konstantinou and T. A. Albanis, *Applied Catalysis B: Environmental,* 2004, **49**, 1.

30. S. M. Ghoreishi, M. Behpour and M. Golestaneh, *Anal. Methods*, 2011, **3**, 2842.

31. R. Jain, M. Mathur, S. Sikarwar and A. Mittal, *Journal of Environmental Management*, 2007, **85(4)**, 956.

32. K. G. Bhattacharyya and A. Sharma, *Dyes and Pigments*, 2005, **65**, 51.

33. P. Wilhelm and D. Stephan, *Journal of Photochemistry and Photobiology A: Chemistry*, 2007, **185**, 19.

34. N. A. Bastaki, *Chemical Engineering and Processing: Process Intensification,* 2004 , **43(12)**, 1561.

35. B. Shi, G. Li, D. Wang, C. Feng and H. Tang, *Journal of Hazardous Materials,* 2007, **143(1-2)**, 567.

36. Y. Gao, D. Shan, F. Cao, J. Gong, X. Li, H. Ma, Z. Su and L. Qu, *J. Phys. Chem. C*, 2009, **113**, 15175.

37. S. Xuan, Y. X. J. Wang, J. C. Yu and K. C. F. Leung, *Langmuir*, 2009, **25(19)**, 11835.

38. M. R. Nabid, R. Sedghi, P. R. Jamaat, N. Safari and A. A. Entezami, *J. Appl. Polym. Sci.,* 2006, **102**, 2929.

39. A. A. Athawale, M. V. Kulkarni and V. V. Chabukswar, *Materials Chemistry and Physics,* 2002, **73**, 106.

40. T. Hino, T. Namiki and N. Kuramoto, *Synth. Met.,* 2006, **156**, 1327.

41. Y. Tang, K. Pan, X. Wang, C. Liu and S. Luo, *Journal of Electroanalytical Chemistry,* 2010, **639**, 123.

42. S. K. Pillalamarri, F. D. Blum, A. T. Tokuhiro and M. F. Bertino, *Chem. Mater.,* 2005, **17**, 5941.

43. R. J. Tseng, C. O. Baker, B. Shedd, J. Huang, R. B. Kaner, J. Ouyang and Y. Yang, Appl. Phys. Lett. 2007, **90**, 053101.

44. M. Aldissi and S. P. Armes, *Macromolecules,* 1992, **25**, 2963.

45. R. R. Naujok, R. V. Duevel and R. M. Corn, *Langmuir,* 1993, **9**, 1771.

46. S. T Sivapalan, B. M Devetter, T. K. Yang, T. Dijk, M. V Schulmerich, P. S. Carney, R. Bhargava and C. J. Murphy, *ACS Nano*, 2013, **7(3)**, 2099.

47. K. Mallick, M. J. Witcomb, M. S. Scurrell, *J. Phys.: Condens. Matter*, 2007, **19**, 196225.

48. Subrata Kundu, *J.Mater.Chem.C*, 2013, **1**, 831.

49. M. M. Ayad and A. A. E. Nasr, *J. Phys. Chem. C,* 2010, **114,** 14377.

50. P. Xiong, L. Wang, X. Sun, B. Xu and X. Wang, *Ind.Eng.Chem.Res.* 2013, **52**, 10105

51. M. Shanthil, R. Thomas, R. S. Swathi and K. G. Thomas, *J. Phys. Chem. Lett.*, 2012, **3**, 1459.

52. B. Zhang, B. Zhao, S. Huang, R. Zhang, P. Xu, H. L.Wang, *Cryst. Eng. Comm.*, 2012, **14**, 1542.

53. Z. Gan, A. Zhao, M. Zhang, W. Tao, Ho. Guo, Q. Gao, R. Mao and Erhu Liu, *Dalton Trans.,* 2013, **42**, 8597.

54. Z. J. Jiang, C. Y. Liu and L. W. Sun, *J. Phys. Chem. B,* 2005, **109**, 1730.